

Behaviour of poorly detailed lap-splices under cyclic loading

G. Angeli¹, P. Hannewald¹, K. Beyer¹

¹ Earthquake Engineering and Structural Dynamics Laboratory (EESD), School of Architecture, Civil and Environmental Engineering (ENAC), École Polytechnique Fédérale de Lausanne (EPFL), Switzerland

Abstract. This paper presents the first part of a series of uniaxial cyclic tests on lap-splices. The work is conducted within the framework of a project on the seismic behaviour of existing, poorly detailed bridge piers which are typically constructed with a lap-splice above the footing. The test series presented here was initiated to study the influence of load history, especially with regards to the compression levels, and confinement on the behaviour of lap-splices. The test units represent the boundary elements of previously tested large scale bridge piers. This paper describes three tests on units with varying transverse reinforcement ratios, which were subjected to the same cyclic load history, in more detail. Particular attention is given to their failure modes and selected measurements, such as slip of the bars and concrete strain levels, are presented.

Keywords: Lap-splices, bridge piers, detailing, cyclic-loading, load history

1 INTRODUCTION

The tests on lap-splices presented in this paper were conducted within the framework of a research project on the seismic safety of existing Swiss bridges. Within this project, the cyclic inelastic behaviour of wall-type bridge piers with detailing deficiencies is investigated especially with regards to the displacement capacity, a reliable estimate of which is required to perform a displacement-based assessment. As many of the existing bridges were built before seismic design provisions were introduced in codes, their detailing does not meet current requirements. Typically, bridge piers were constructed with lower transverse reinforcement ratios than required for capacity design, without confined boundary elements and with lap-splices at the bottom of the pier, where the plastic hinge is expected to develop. A series of quasi-static cyclic tests on bridge piers with the mentioned deficiencies was conducted to create an experimental database for the project (Bimschas 2010, Hannewald et al. 2013). Three piers tested in this series were constructed with lap-splices at the base. Two of them started to lose their load bearing capacity when the concrete surrounding the lap-splices at the outer edge of the pier was crushed in compression. The third one developed splitting cracks along the splices before any compression damage of the concrete was visible. To study the behaviour of splices under cyclic loading in more detail, especially with regards to their failure mechanisms and the limit strains triggering the failure, a test series on specimens representing the boundary regions of the previously tested large-scale piers is conducted. . The paper outlines the scope of the test series, describes the characteristics of the test units and the applied load history (Section 2). It also presents selected results of the first three tests (Section 3).

2 EXPERIMENTAL PROGRAM

2.1 Background

This experimental campaign is conducted in order to examine the influence of load history and confinement on lap splices. For this reason, specimens with different confining reinforcement ratios are tested uniaxially subjected to varying load histories. After a small series of preliminary tests, which were used to check test setup and instrumentation, three different test unit layouts, which will be described in Section 2.2, and four load histories were defined. This paper describes three tests with different layouts, which were subjected to the same reversed cyclic load history presented in Section 0.

2.2 Characteristics of the test units

The test units are 650mm high and have a square section of $350 \times 350 \text{mm}^2$, see Figure 1. Each test unit contains eight splices, four in the front and four at the back. The diameter of the longitudinal bars is $d_l=14\text{mm}$ and the length of the splices is $600\text{mm} \sim 43d_l$, which also was the length of the splices of the corresponding bridge pier test units. The outer dimensions, the longitudinal spliced reinforcement and the splice length are equal in all test units. The test units differ only with respect to the transverse reinforcement which consisted of stirrups with a diameter of 6mm. Three different layouts have been chosen: Four stirrups with 180mm spacing (layout L1), six stirrups with 110mm spacing (layout L2) and eight stirrups with 75mm spacing (layout L3). The main characteristics of the specimens are presented in Table 1.

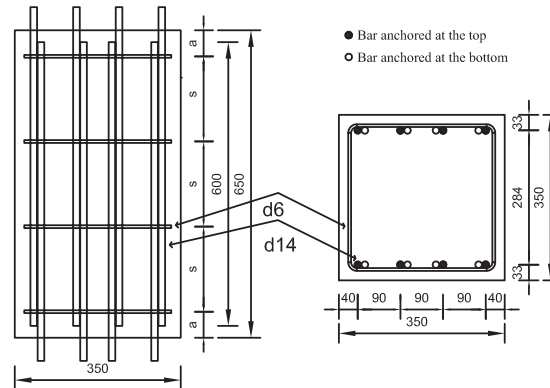


Figure 1 Layout and details of the test units

Table 1. Characteristics of the test units

Test unit		L1	L2	L3
Dimension $b / h / l$	[m]	0.35/0.35/0.65	0.35/0.35/0.65	0.35/0.35/0.65
Spliced reinforcement	[mm]	$8 \times 2 \times d_{14}$	$8 \times 2 \times d_{14}$	$8 \times 2 \times d_{14}$
Longitudinal reinforcement ratio	[%]	1.01	1.01	1.01
Lap splice length	[-]	600mm \sim 43d _l	600 mm \sim 43d _l	600 mm \sim 43d _l
Transverse reinforcement	[mm]	$4 \times d_6$	$6 \times d_6$	$8 \times d_6$
Transverse reinforcement ratio	[%]	0.10	0.15	0.20
Stirrup spacing - detail (s) Fig. 1	[mm]	180	110	75
Stirrup spacing - detail (a) Fig. 1	[mm]	55	50	63

2.3 Material properties

2.3.1 Concrete

A standard mix of concrete of compression strength class C25/30 was used. The maximum aggregate size was 16mm and the water cement ratio was 0.5 with 310kg/m³ cement of class 42.5N. It was designed to resemble the concrete used for the large scale bridge piers tests. Table 2 presents the results obtained from the material tests. Three cylinders of 150 mm diameter and 300 mm height were used to determine the compression strength. The modulus of elasticity was determined based on a procedure similar to that suggested in SIA 162/1 (1989), as tangent modulus in the third cycle between 1MPa and 12MPa. To obtain the tensile strength, double punch tests on concrete cylinders with a diameter of 150mm and a height of 150mm were performed. The tensile strength was then calculated according to Chen (1980).

Table 2 Concrete properties

Property	f_c MPa	f_{ct} MPa	E_c GPa	ε_c ‰
Concrete	42.0	2.9	13.9	2.5
Large scale test	28.2			1.0

To study the scaling effect between the standard cylinders used for the compression test and the large scale test units, a concrete block of the same dimensions as the latter was tested in compression. The compression strength f_c of this test unit was 28.2MPa and thus 32% lower than the average strength of the concrete cylinders. An average strain at peak stress of $\varepsilon_c = 1‰$ was measured between the two rows of LEDs at $z=150\text{mm}$ and 450mm (coordinate z measured from the bottom lap splice), see Figure 3. This area was considered to be sufficiently far from the loading plates, which provide a lateral restraint, to yield a good measure for the average strain of the test unit. The strains determined with these two rows of LEDs will also be used later in Figure 7, Figure 10 and Figure 13. For comparison with the cylinder tests, the material properties obtained from the large scale test are also listed in Table 2.

2.3.2 Steel

Steel tests on six samples each were carried out to determine the properties of the longitudinal reinforcement and the stirrups. A ductile steel of “type Topar - S500C” was used for the longitudinal reinforcement and cold-formed, micro-alloyed steel for the stirrups. With these tests, the modulus of elasticity E_s , the yield and ultimate strength f_y and f_u , as well as strain at the maximum force ε_{sy} , presented in Table 3, were determined. For the d6 bars, which did not have a yield plateau, the proof strength at 2‰ non proportional extension was determined instead of the yield strength.

Table 3 Steel properties

Steel	E_s GPa	f_y MPa	f_u MPa	ε_u ‰
Samples : 6				
d14	192	511	628	135
d6	212	485	609	81

2.4 Test set up and instrumentation

2.4.1 Test set up

The tests described in this paper were uniaxial quasi-static cyclic tests in which tension was applied to the bars and compression to the concrete. The longitudinal reinforcement bars were elongated with threaded bars that were fixed to steel plates with which tension was applied. Load cells were inserted

at the top of the longitudinal reinforcement to directly measure the tensile force in each bar, as illustrated in Figure 2. Compression was applied through layers of steel plates that were straightened and carefully aligned to ensure uniform load application.

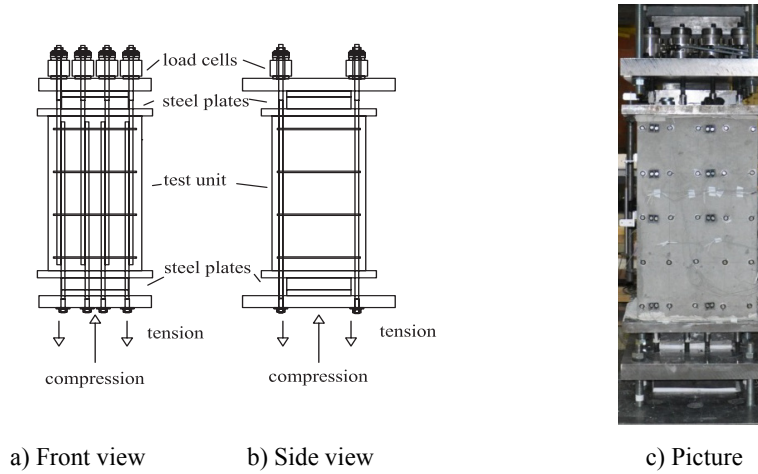


Figure 2 Test set up

2.4.2 Instrumentation

The instrumentation of the test units with strain gages, LVDTs and LEDs is presented in Figure 3. The strain in the reinforcement was measured with strain gages glued onto the bars. One of the splices in the centre was instrumented with four strain gages on each bar as shown in Figure 3a and b. Furthermore, four stirrups were instrumented with strain gages right above the lap splices in the corner. To measure the deformations on the surface, two rows of LVDTs were mounted at the back of the test unit, as shown in Figure 3c. Moreover, LEDs were glued along a regular pattern on the concrete as well as on the longitudinal bars, as illustrated in Figure 3d. With these, the deformations at the surface of the test unit and the slip of the lap-splices were tracked using an optical measurement system. Furthermore, complementary to the strain gages, which measure the strain at a certain location, the LEDs allow for calculating the average strain over a larger distance between two LEDs.

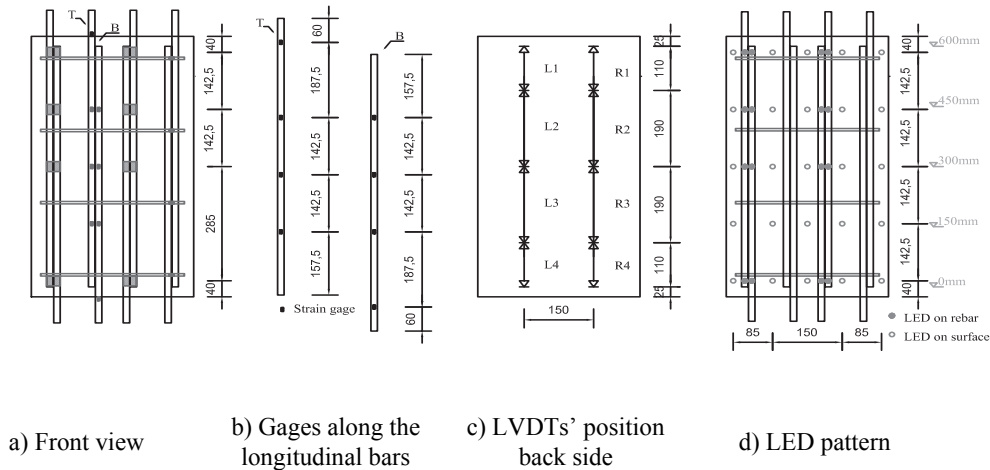


Figure 3 Instrumentation

2.5 Load history

The load history is based on strains measured near the base of the corresponding bridge pier tests (Hannewald et al. 2013), where the reinforcement was spliced. These strains were used to define compression levels, while a constant tension force level was chosen for simplicity. Corresponding to the pier tests, two cycles to compression strain levels of 0.25, 0.5, 1, 1.5 and 2‰ were defined, see Figure 4. As it was not deemed feasible to find one measurement that represented well the average strain of the entire test unit and could thus be used to control the test, the strain levels were converted to force levels, which defined the amplitudes of the cycles. To compute the force levels, a modified formulation based on Popovic's (1970) proposal for the stress-strain relationship of concrete was used in combination with the cylinder strength of the concrete. The tension force amplitude was constant throughout all cycles at 90% of the yielding force of the longitudinal bars. Usually, failure in compression was reached first, after which the test unit was loaded to failure in tension.

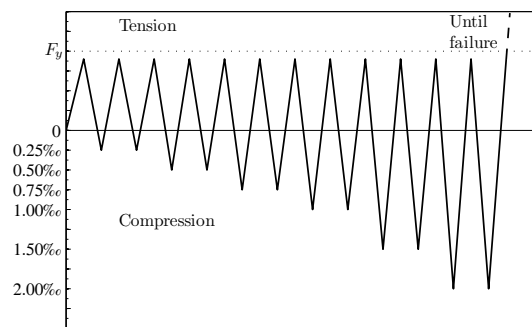
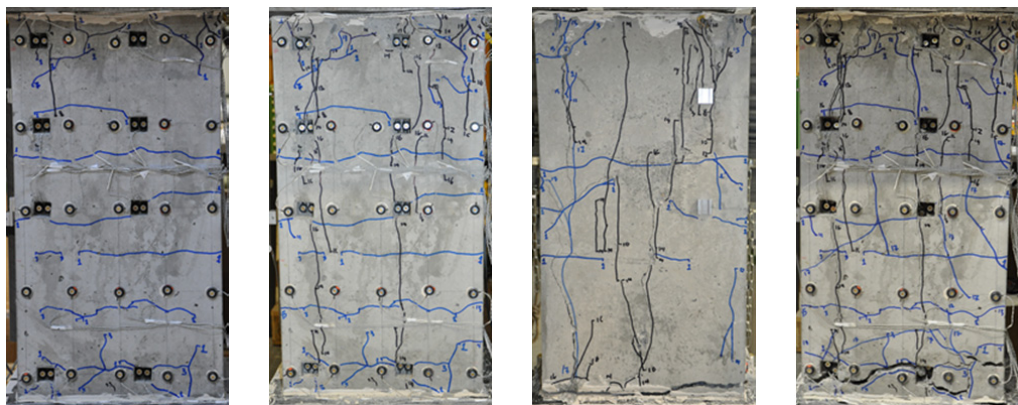


Figure 4 Load history graph

3 TEST RESULTS

3.1 Test unit with layout 1 (L1)

The loading phase follows the history presented in Figure 4. At the first tensile load step, at 90% of the yielding force of the longitudinal reinforcement bars, the first tensile cracks formed in the vicinity of the stirrups. At the second loading to 0.5‰ compression strain, the first compression crack at the front side of the specimen appeared (marked black in Figure 5a).



a) First compression crack

b) Compression failure crack

c) Side splitting

d) Tensile failure crack

Figure 5 Pictures at different load levels

During the following compression half-cycles, more compression cracks developed, whereas there was little progression of tensile cracking after the first load step. At the first load step at 1‰ compression strain, the first compression crack running from the bottom to the top of the test unit occurred. The maximum compression force applied to the test unit was 3349kN, corresponding to 27.3MPa, at the first strain level of 1‰. During the second cycle to 1‰ peak strain, the load started to drop after 3287kN were reached, which means that compression failure occurred, see Figure 5b. The average strain at this peak compression load, measured with the second and third row of LVDTs at the back, was 1.05‰. Compression cracks developed all around the specimen. After failure in compression, the test unit was loaded to failure in tension. During this loading in tension, a maximum force of 577kN was reached before the bars began to slip significantly and the load thus dropped. That means failure occurred before all bars attained the yield load, which sums up to a total force of 630kN. Splitting cracks developed along the spliced region at the sides of the test unit (Figure 5c). The slip between two bars of the same splice was large enough to be visible by eye from the position of the LEDs (Figure 5d). The strains that developed along the longitudinal bars of the splices in the corner and the centre of the test unit are presented in Figure 6 where “top” and “bottom” refer to the the reinforcement bar that was anchored at the top and bottom of the test unit, respectively.

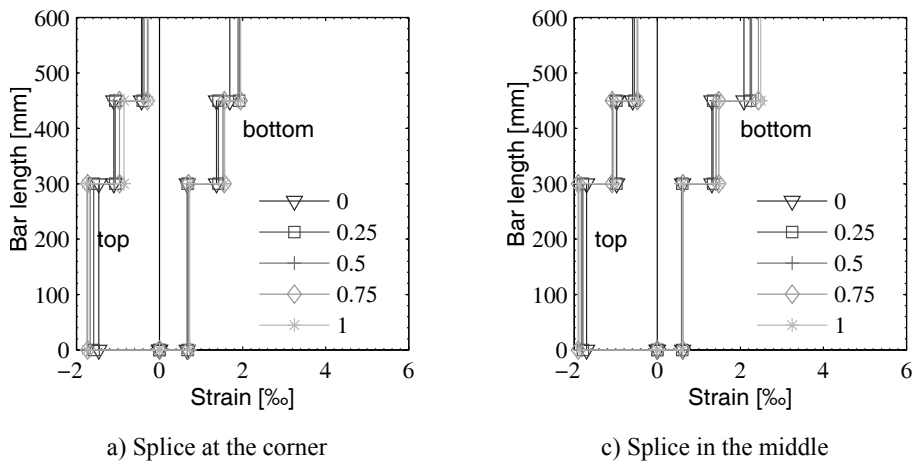


Figure 6 Longitudinal bar strain

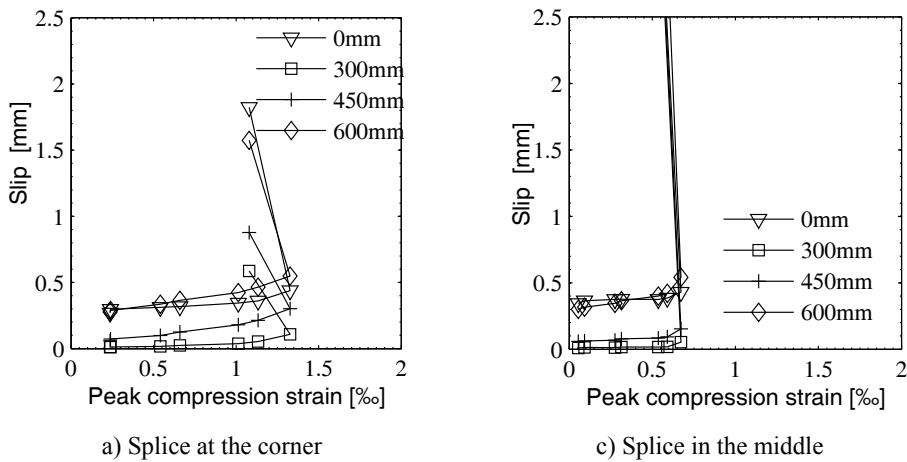


Figure 7 Peak compression strain at different load steps and bar slip at the next LS

These strains, calculated with a relatively large base length from the LEDs on the reinforcing bars, do not indicate a significant redistribution of strains and thus stresses throughout the test within each

splice. The peak compression strain and the slip along the bar at the next tensile load step is presented in Figure 7. The compression strains in this plot were determined with the LEDs that were closest to the corresponding splice, i.e. the slip is plotted against a local strain and not an average one. There was little development of slip in both instrumented splices before the test unit failed in tension.

3.2 Test unit with layout 2 (L2)

The transverse reinforcement content of test unit L2 was 50% higher than for L1. The load was again applied according to Figure 4. As previously, the first tensile cracks in vicinity of the stirrups formed during the initial tensile loading. The first compression cracks developed during the second cycle to 0.75‰ at the front side of the unit when the load reached 3388kN, which corresponds to 27.7MPa compression stress (Figure 8a).

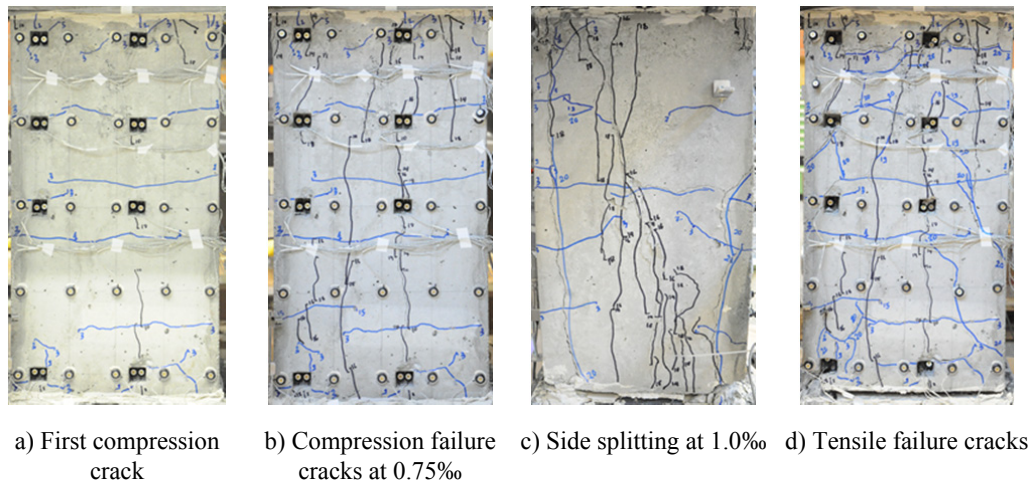


Figure 8 Pictures at different load levels

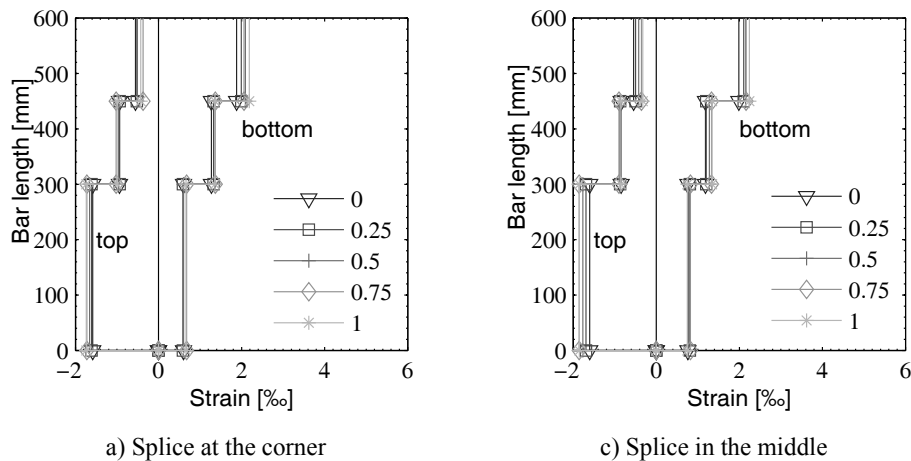


Figure 9 Longitudinal bar strain

At the second cycle, the first compression crack that went from bottom to top was visible. In the next compression cycle to 1‰ the load started dropping after 3378kN were reached, accompanied by the formation of cracks all around the specimen (Figure 8 Pictures at different load levels

b). After this failure in compression, the test unit was again loaded to failure in tension. Tensile failure occurred at 645kN, which corresponds to 1.02 times the yield force and is thus greater than the tensile

force of $0.90F_y$, reached at every tensile load step. Splitting cracks (marked blue in Figure 8c&d) formed close to most lap splices and significant slipping of the bars was visible. Once again, the strain which developed along the longitudinal bars of the splices at the corner and in the middle of the unit as well as the peak compression strain levels and the slip along the bar at the next tensile load step are presented in Figure 9 and Figure 10. As we can see, there is no significant redistribution of strains and thus stresses within each splice throughout the test, similar to the first test unit (Figure 9). Moreover, there was little development of slip in both instrumented splices before the test unit failed in tension (Figure 10). The slip at the splice in the middle of the test unit at the last load step was greater than the slip of the splice at the corner.

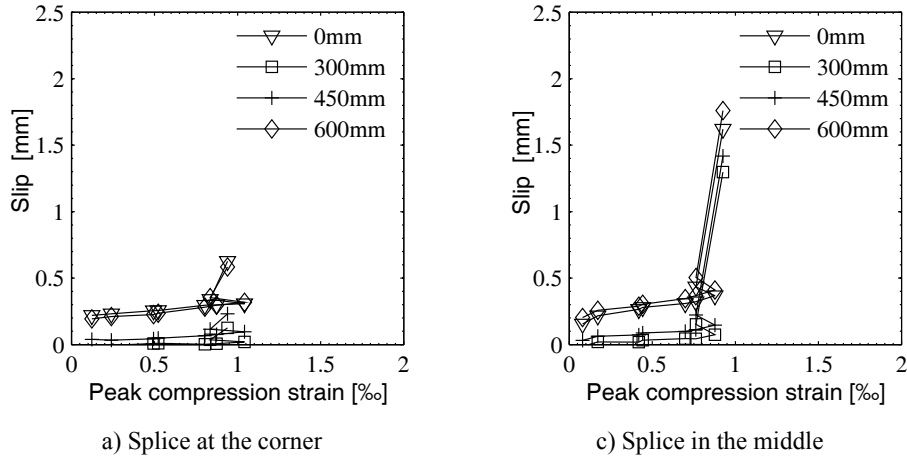


Figure 10 Peak compression strain at different load steps and bar slip at the next LS

3.3 Test unit with layout 3 (L3)

The last test unit is the one which contained the highest amount of stirrups and was loaded the same way as the two previous ones. The first tensile cracks were visible in the vicinity of the stirrups during the first load step in tension. The first compression crack appeared at the first cycle of the 0.75‰ strain level, see Figure 11a where it is marked in black.

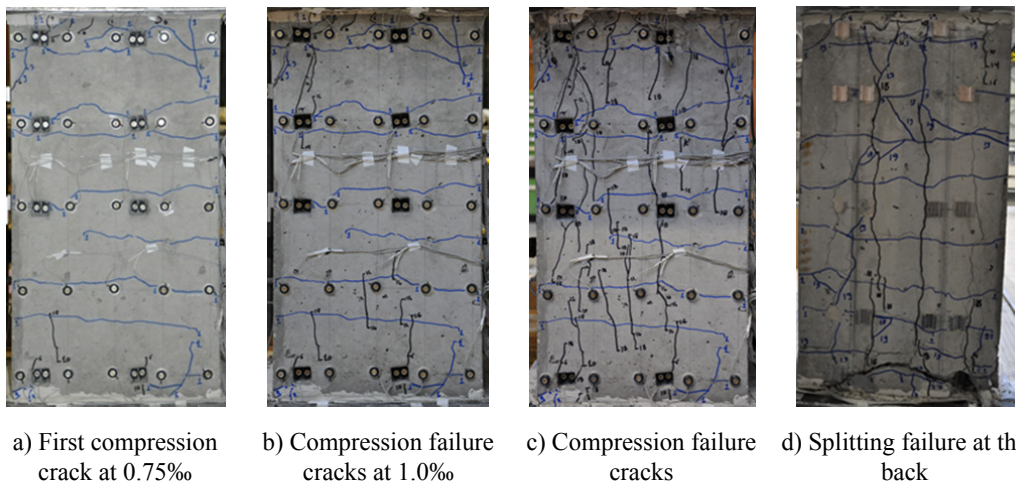


Figure 11 Pictures at different load levels

Some more extensive compression cracking occurred at the second cycle of 1% strain level (Figure 11b). At this load step, the previous two test units had failed in compression already. Failure of this test unit in compression eventually occurred during the first loading to 1.5% strain level, at a load of 3713kN, corresponding to 30MPa stress. Compression cracks formed all around the specimen, see Figure 11c. Following the compression failure, tensile loading was applied up to failure, which occurred at a load of 518kN, i.e. at 91% of the force applied at every tensile load step. Extensive splitting cracking as well as slipping of the spliced bars was visible at this point, see Figure 11c. The strain that developed along the longitudinal bars at the corner and in the middle of the test unit as well as the peak compression strain levels and the relative slip between the two bars of a splice at the next tensile load step are presented in Figure 12 and Figure 13, respectively.

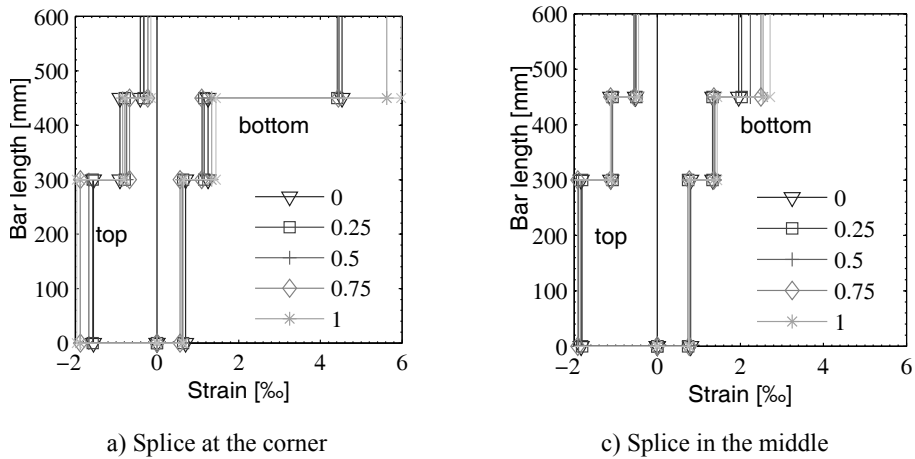


Figure 12 Longitudinal bar strain

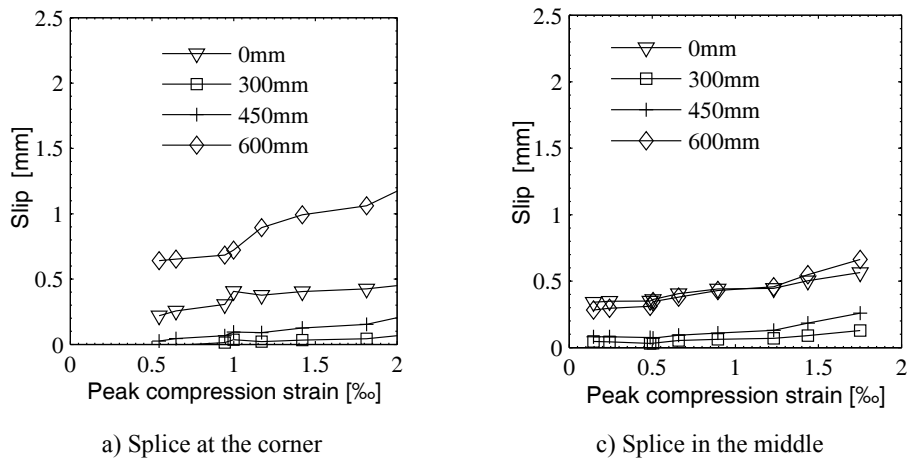


Figure 13 Peak compression strain at different load steps and bar slip at the next LS

Once again, there was no significant redistribution of strains within each splice throughout the test. Figure 13 shows that, contrary to the previous tests, the slip develops more evenly throughout the test in both instrumented splices before the test unit failed in tension. Comparison with the previous results shows that the strains of this test unit, which had the largest transverse reinforcement ratio, were much higher than before. While the tensile failure with significant slipping occurred after approximately 1.0% strain were measured in the other tests, this test unit displays a steadier, slow increase of slip up to around 2.0% compression strain, before tensile failure.

3.4 Summary of results

The main observations with regards to the load and strain of the above described tests are presented in Table 4. It summarises the maximum forces and stresses in compression, f_c as well as the corresponding strains and the cycle at which compression failure occurred and the forces and stresses in tension prior to failure in tension f_t . The strains were measured with the two rows of LEDs at 150mm and 450mm height around the instrumented bars at the corner $\epsilon_{c,c}$ and in the middle $\epsilon_{c,m}$ of the test unit, i.e. they correspond to those used in the figure displaying the development of slip in the previous sections. With regards to a possible redistribution of strains and stresses along the splice due to the cyclic loading, the previously shown data indicates no significant redistribution. Furthermore, the previously included figures presenting the peak compression strain at different load steps and the bar slip at the next load step for each test unit indicate that there was little development of slip in the two test units with the lower transverse reinforcement ratios. On the contrary, the test unit with the highest transverse reinforcement ratio exhibited a continuous growth of slip. The latter test unit also developed the highest strains.

Table 4 Main observations for each layout

Layout	F_c kN	f_c MPa	F_t kN	f_t MPa	$\epsilon_{c,c}$ ‰	$\epsilon_{c,m}$ ‰	Compression failure at cycle
L1	3349	27.3	577	469	1.10	0.50	2 nd 1‰
L2	3388	27.6	645	524	0.95	0.93	1 st 1.5‰
L3	3713	30.3	518	421	2.20	1.80	1 st 1.5‰

4 CONCLUSIONS AND OUTLOOK

To study the effect of the number of cycles of pre-compression in the tensile failure of the lap splices a second test series is going to follow. Monotonic tests to study the effect of pre-compression on the tensile failure and vice versa are going to conclude this experimental programme. The final objective is to derive limit strains as a function of load history and transverse reinforcement that characterise the onset of lap splice failure.

ACKNOWLEDGEMENTS

The study presented in this paper has been carried out in the framework of a research project funded by the Swiss Federal Roads Office (FEDRO) with project number AGB 2008/001. This financial support is gratefully acknowledged.

REFERENCES

- Bimschas, M. (2010). *Displacement-Based Seismic Assessment of Existing Bridges in Regions of Moderate Seismicity*, IBK Report 326, Swiss Federal Institute of Technology ETH, Zurich, Switzerland
- Chen, W.F., Yuan, R.L. (1980) Tensile strength of concrete: Double-punch test, *ASCE Journal of the Structural Division*, **106**, 1673–1693
- Hannewald, P., Bimschas, M. and Dazio, A. (2013). *To be published: Quasi-static cyclic tests on RC bridge piers with detailing deficiencies*, IBK Report, Swiss Federal Institute of Technology ETH, Zurich, Switzerland
- Popovics, S. (1970) A Review of Stress-Strain Relationships for Concrete, *ACI Journal*, **67**, 243-248.
- SIA 162/1 (1989) *Betonbauten Materialprüfung, (Concrete structures, material tests)* Swiss Society of Engineers and Architects, Zurich, Switzerland